CHAPTER 11

RESULTS

As described in Chapter 10, the `Combine` tool is used to perform the likelihood fits from which we extract the results of this analysis. Before performing the likelihood fits to the data, we first perform the fits with asimov data that corresponds to the SM expectation. These blinded asimov fits allow us to determine the expected sensitivity and perform optimization studies without introducing biases; for example, the sensitivity optimization described in Section 6.3 was performed using only asimov data. The results of the asimov fits are shown in Section 11.1. The unblinded results of this analysis (from the fits to the observed data) are reported in Section 11.2. The results are found to be consistent with the SM expectation. Some visualizations of the results (2-dimensional scans and post-fit histograms) are included in Section 11.3.

It should be noted that after unblinding this analysis, there were no signs of problematic discontinuities or false minima, so the random starting point approach (described in Section 10.3) was not used to obtain the final results. The 1-dimensional profile scans in this analysis exhibit fewer double minima than were observed in [32] (the predecessor to this analysis), which could be due to degeneracies that have been broken by the improvements implemented in this iteration; the fact that there are fewer local minima may help to explain why the profiled fits in this analysis seem to be able to successfully navigate the space and find the true minima without the need for random starting points. However, it is difficult to know a priori whether or not the fits will be susceptible to local minima, so future analyses should keep this challenge in mind when performing profiled likelihood scans.

11.1 SM expected limits

The 1-dimensional likelihood scans are shown for each WC in Figure 11.1; the other 25 WCs are either profiled (shown by the black markers) or fixed at their SM values of zero (shown by the red markers). As explained in Section 10.1, the 1σ and 2σ confidence intervals can be read off of these scans by observing where the 2ΔNLL curve crosses 1 and 4, respectively. The resulting 1σ and 2σ confidence intervals are listed in Table 11.1 and displayed in Figure 11.2. Since these scans are performed with asimov data, they represent the expected sensitivity of the analysis under the SM hypothesis.

11.2 Observed results

The 1-dimensional likelihood scans are shown for each WC in Figure 11.3; the other 25 WCs are either profiled (shown by the black markers) or fixed at their SM values of zero (shown by the red markers). The resulting 1σ and 2σ confidence intervals are listed in Table 11.1 and displayed in Figure 11.2. The results are consistent with the SM prediction.

11.3 Visualization of results: 2-dimensional scans and postfit summary histograms

In Section 11.2, we explored the likelihood along 1-dimensional directions of the full 26-dimensional surface. In principle, it would be interesting to study the shape of the full 26-dimensional surface; however, in practice it is very difficult to explore high-dimensional spaces. In lieu of the full 26-dimensional visualization, we can at least explore 2-dimensional slices of the space. Similar to the 1-dimensional scans described above, we scan over two WCs and profile the remaining 24 WCs. The 2-dimensional scans are useful for identifying WCs that are correlated; for example Figure 11.5 shows a strong correlation between the c_{tW} and c_{tZ} WCs.

To visualize the results in a different way, we can compare histograms (for the categories and bins in the analysis) of the observed yields and the predicted yields. The top figure in Figure 11.6 shows the observed data compared against the SM prediction. In this "prefit" case, we have evaluated the 26-dimensional quadratic (that parametrizes the predicted yields in terms of the WCs) at the SM value of zero for each WC. In other words, we have reweighted the prediction to the SM. In the bottom figure of Figure 11.6, the prediction has been reweighted to the best fit point (as obtained from the likelihood fits). This is referred to as the "postfit" scenario. The shaded bands in the plots represent the total uncertainty, and it can be seen that in both the prefit and postfit scenarios, the observation is within the uncertainty on the prediction for most of the bins in the analysis; this visualization is consistent with the results of the statistical analysis, which found the SM point to be consistent with the data.

TODO: If we end up figuring out anything else to say about the results and/or visualization, add that into this section (or into a new section)

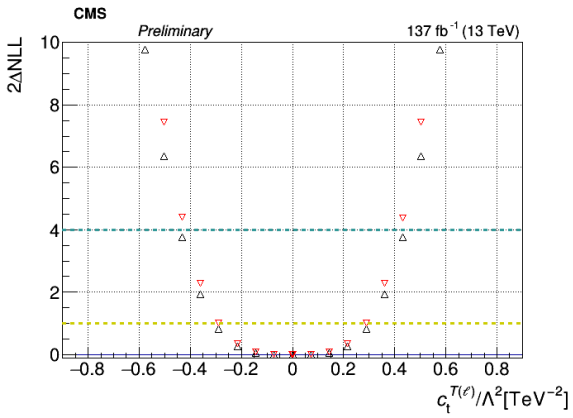
CMS
Preliminary
137 fb^{-1} (13 TeV)
2ΔNLL
$c_t^{T(\ell)}/\Lambda^2[\text{TeV}^{-2}]$

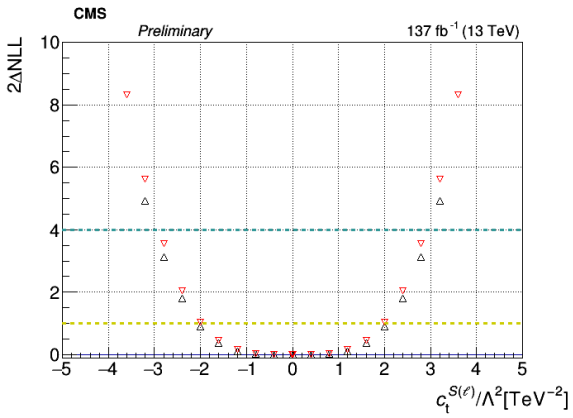
CMS
Preliminary
137 fb^{-1} (13 TeV)
2ΔNLL
$c_t^{S(\ell)}/\Lambda^2[\text{TeV}^{-2}]$

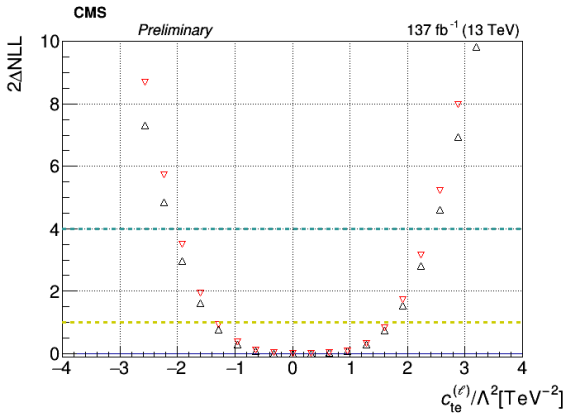
CMS
Preliminary
137 fb^{-1} (13 TeV)
2ΔNLL
$c_{te}^{(\ell)}/\Lambda^2[\text{TeV}^{-2}]$

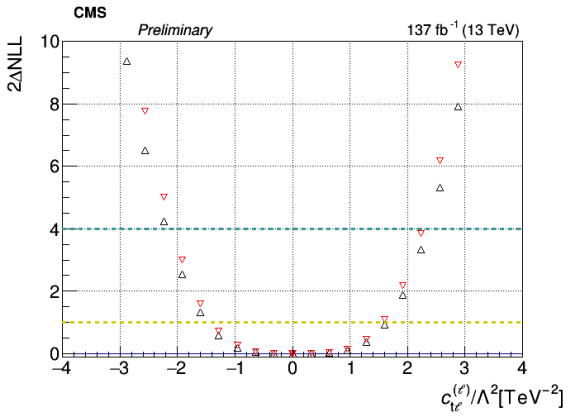
CMS
Preliminary
137 fb^{-1} (13 TeV)
2ΔNLL
$c_{t\ell}^{(\ell)}/\Lambda^2[\text{TeV}^{-2}]$

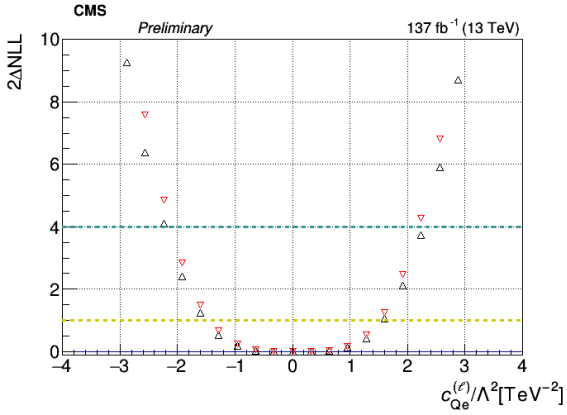
CMS
Preliminary
137 fb^{-1} (13 TeV)
2ΔNLL
$c_{Qe}^{(\ell)}/\Lambda^2[\text{TeV}^{-2}]$

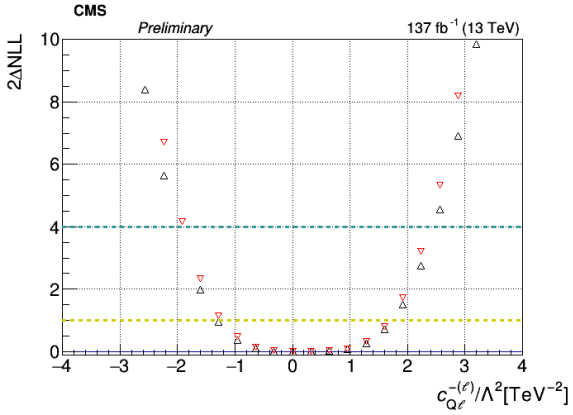
CMS
Preliminary
137 fb^{-1} (13 TeV)
2ΔNLL
$c_{Q\ell}^{-(\ell)}/\Lambda^2[\text{TeV}^{-2}]$

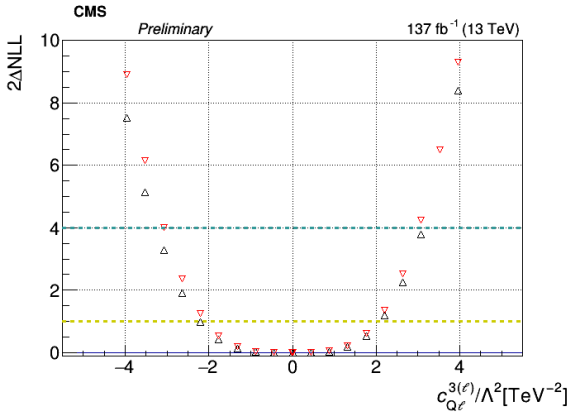
CMS
Preliminary
137 fb^{-1} (13 TeV)
2ΔNLL
$c_{Q\ell}^{3(\ell)}/\Lambda^2[\text{TeV}^{-2}]$

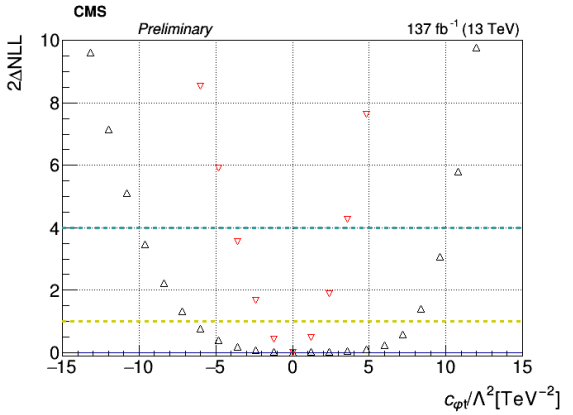
CMS
Preliminary
137 fb^{-1} (13 TeV)
2ΔNLL
$c_{\varphi t}/\Lambda^2[\text{TeV}^{-2}]$

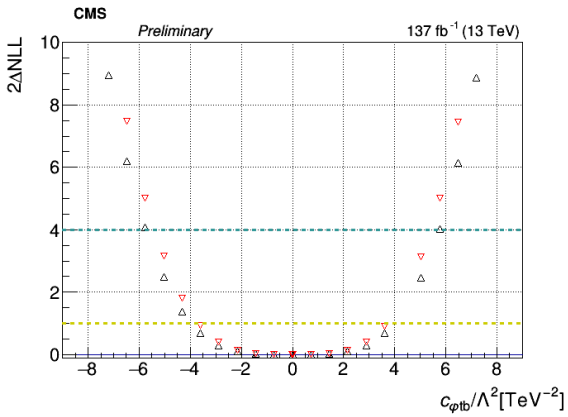
CMS
Preliminary
137 fb^{-1} (13 TeV)
2ΔNLL
$c_{\varphi tb}/\Lambda^2[\mathrm{TeV}^{-2}]$

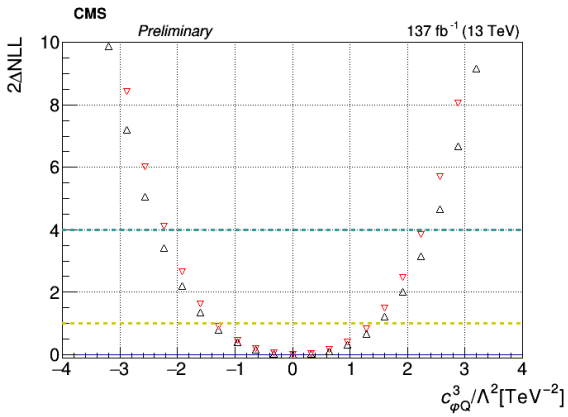
CMS
Preliminary
137 fb^{-1} (13 TeV)
2ΔNLL
$c^3_{\varphi Q}/\Lambda^2[\mathrm{TeV}^{-2}]$

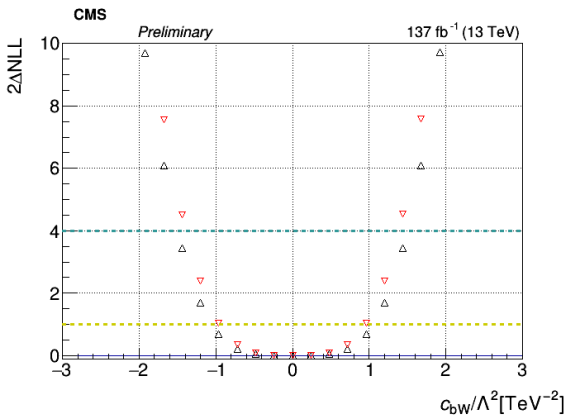
CMS
Preliminary
137 fb^{-1} (13 TeV)
2ΔNLL
$c_{bW}/\Lambda^2[\mathrm{TeV}^{-2}]$

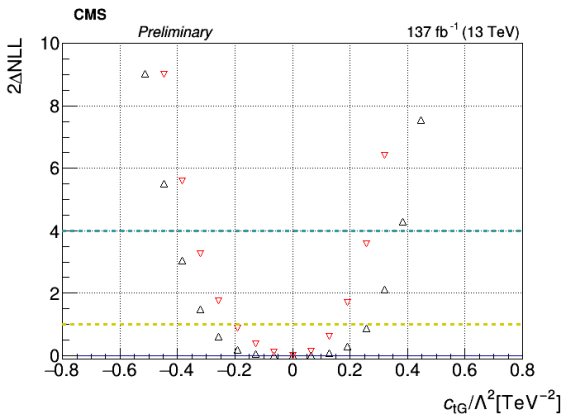
CMS
Preliminary
137 fb^{-1} (13 TeV)
2ΔNLL
$c_{tG}/\Lambda^2[\mathrm{TeV}^{-2}]$

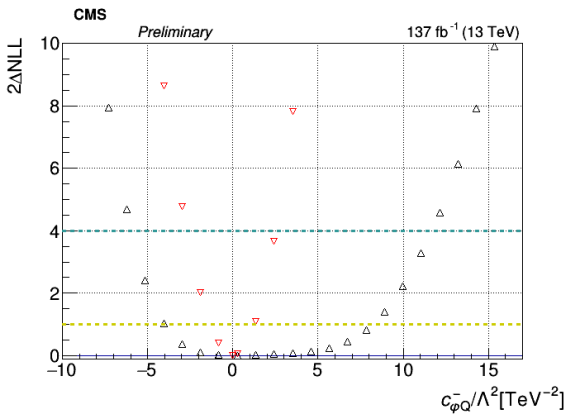
CMS
Preliminary
137 fb^{-1} (13 TeV)
2ΔNLL
$c^-_{\varphi Q}/\Lambda^2[\mathrm{TeV}^{-2}]$

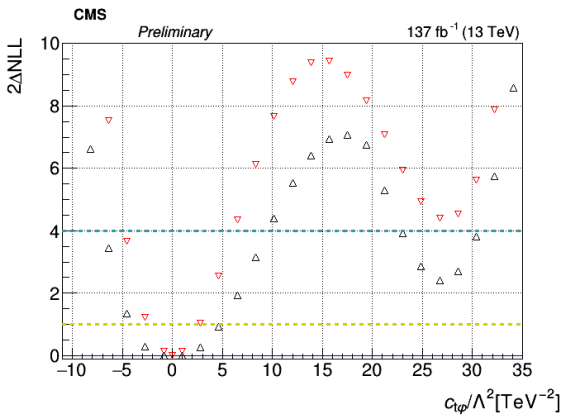
CMS
Preliminary
137 fb^{-1} (13 TeV)
2ΔNLL
$c_{t\varphi}/\Lambda^2[\mathrm{TeV}^{-2}]$

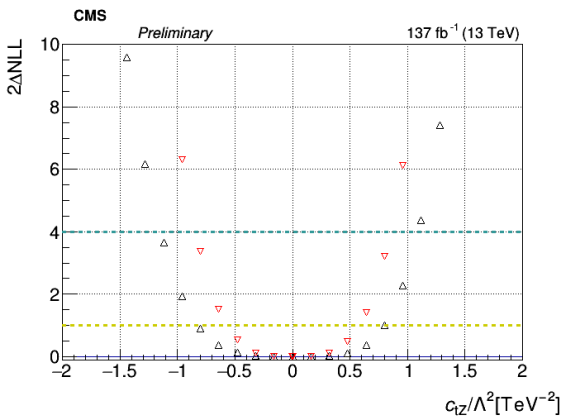
CMS
Preliminary
137 fb^{-1} (13 TeV)
2ΔNLL
$c_{tZ}/\Lambda^2[\mathrm{TeV}^{-2}]$

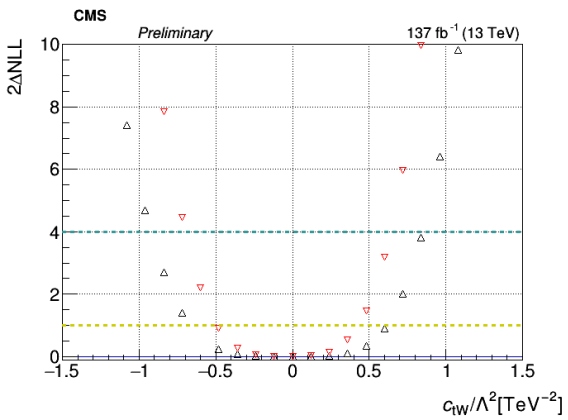
CMS
Preliminary
137 fb^{-1} (13 TeV)
2ΔNLL
$c_{tW}/\Lambda^2[\mathrm{TeV}^{-2}]$

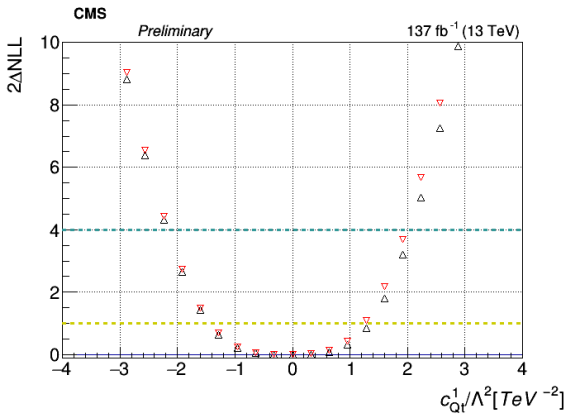
CMS
Preliminary
137 fb^{-1} (13 TeV)
2ΔNLL
$c^{1}_{Qt}/\Lambda^2[TeV^{-2}]$

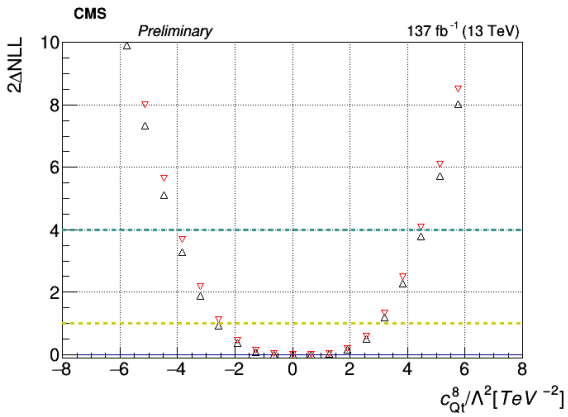
CMS
Preliminary
137 fb^{-1} (13 TeV)
2ΔNLL
$c^{8}_{Qt}/\Lambda^2[TeV^{-2}]$

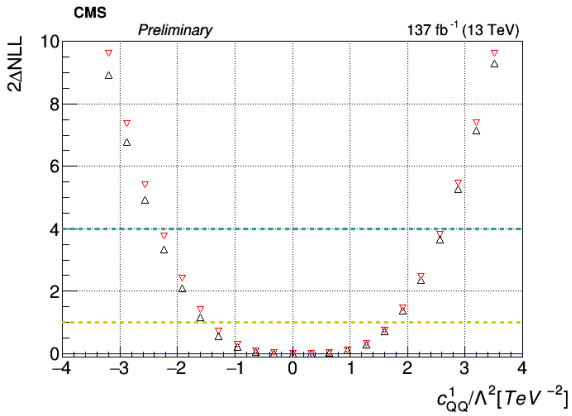
CMS
Preliminary
137 fb^{-1} (13 TeV)
2ΔNLL
$c^{1}_{QQ}/\Lambda^2[TeV^{-2}]$

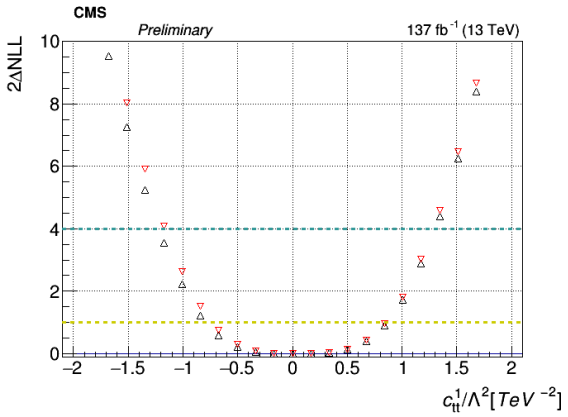
CMS
Preliminary
137 fb^{-1} (13 TeV)
2ΔNLL
$c^{1}_{tt}/\Lambda^2[TeV^{-2}]$

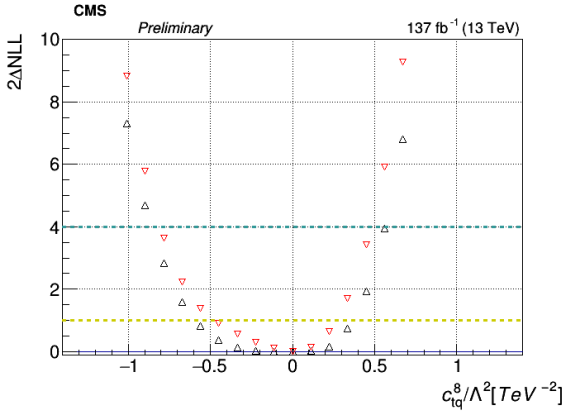
CMS
Preliminary
137 fb^{-1} (13 TeV)
2ΔNLL
$c^{8}_{tq}/\Lambda^2[TeV^{-2}]$

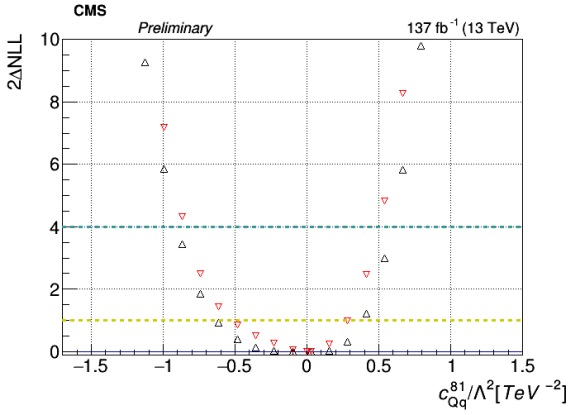
CMS
Preliminary
137 fb^{-1} (13 TeV)
2ΔNLL
$c^{81}_{Qq}/\Lambda^2[TeV^{-2}]$

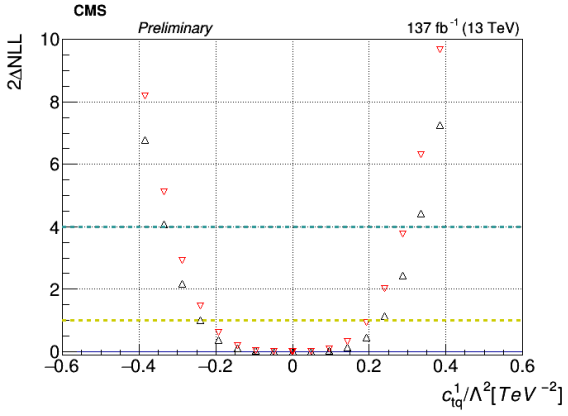
CMS
Preliminary
137 fb^{-1} (13 TeV)
2ΔNLL
$c^{1}_{tq}/\Lambda^2[TeV^{-2}]$

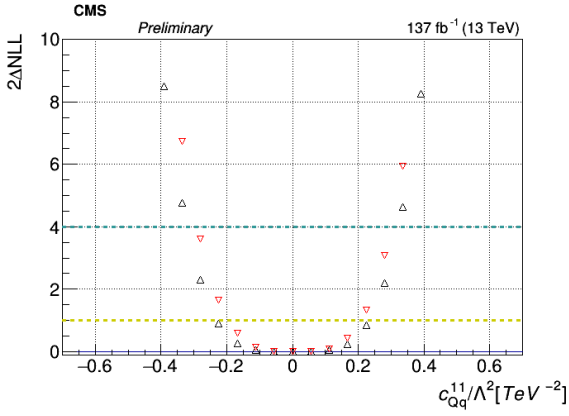
CMS
Preliminary
137 fb^{-1} (13 TeV)
2ΔNLL
$c^{11}_{Qq}/\Lambda^2[TeV^{-2}]$

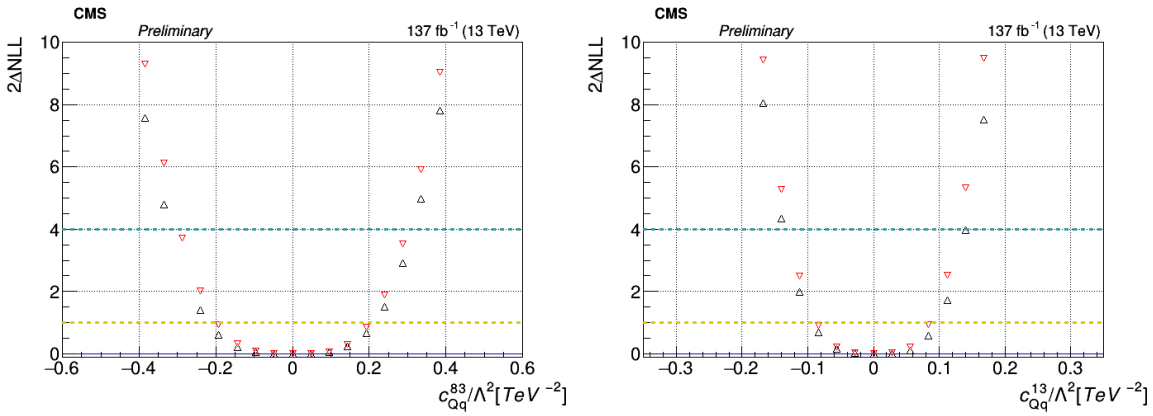

Figure 11.1. SM-expected 2ΔNLL values for 1-dimensional scans for each WCs. The 2ΔNLL values represented in black correspond to the case where the other WCs are profiled, while the 2ΔNLL values represented in red correspond to the case where the other WCs are fixed at their SM values of zero.

TABLE 11.1

SM-EXPECTED 2σ UNCERTAINTY INTERVALS FOR THE 1D SCANS.

WC/Λ^2 [TeV^{-2}]	2σ Interval (others profiled)	2σ Interval (others fixed to SM)
$c_t^{T(\ell)}$	[-0.44, 0.44]	[-0.42, 0.42]
$c_t^{S(\ell)}$	[-3.00, 3.00]	[-2.89, 2.89]
$c_{te}^{(\ell)}$	[-2.10, 2.45]	[-1.99, 2.37]
$c_{t\ell}^{(\ell)}$	[-2.20, 2.35]	[-2.08, 2.26]
$c_{Qe}^{(\ell)}$	[-2.22, 2.28]	[-2.11, 2.19]
$c_{Q\ell}^{-(\ell)}$	[-1.95, 2.46]	[-1.89, 2.36]
$c_{Q\ell}^{3(\ell)}$	[-3.25, 3.12]	[-3.08, 3.02]
$c_{\varphi t}$	[-9.99, 10.01]	[-3.83, 3.47]
$c_{\varphi tb}$	[-5.73, 5.75]	[-5.37, 5.38]
$c_{\varphi Q}^3$	[-2.36, 2.42]	[-2.22, 2.27]
c_{bW}	[-1.49, 1.49]	[-1.38, 1.38]
c_{tG}	[-0.41, 0.38]	[-0.34, 0.27]
$c_{\varphi Q}^-$	[-5.90, 11.65]	[-2.68, 2.51]
$c_{t\varphi}$	[-6.73, 9.58] and [22.92, 30.58]	[-4.73, 6.13]
c_{tZ}	[-1.14, 1.09]	[-0.83, 0.84]
c_{tW}	[-0.92, 0.85]	[-0.70, 0.64]
c_{Qt}^1	[-2.18, 2.06]	[-2.16, 1.97]
c_{Qt}^8	[-4.09, 4.55]	[-3.94, 4.45]
c_{QQ}^1	[-2.37, 2.63]	[-2.29, 2.60]
c_{tt}^1	[-1.22, 1.30]	[-1.17, 1.28]
c_{tq}^8	[-0.85, 0.56]	[-0.80, 0.47]
c_{Qq}^{18}	[-0.90, 0.59]	[-0.85, 0.50]
c_{tq}^1	[-0.33, 0.33]	[-0.31, 0.29]
c_{Qq}^{11}	[-0.32, 0.32]	[-0.29, 0.30]
c_{Qq}^{38}	[-0.31, 0.31]	[-0.29, 0.30]
c_{Qq}^{31}	[-0.14, 0.14]	[-0.13, 0.13]

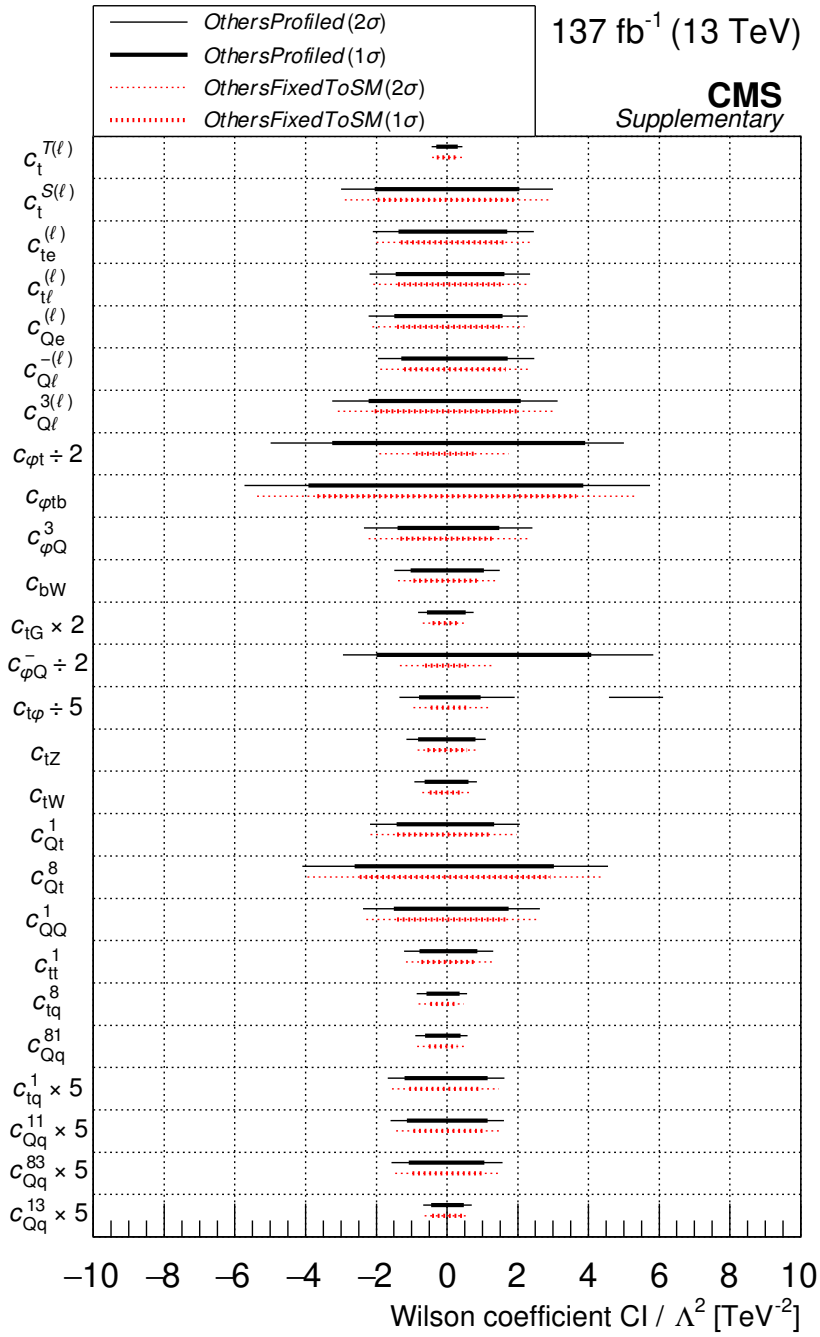

Figure 11.2. Summary of limits from asimov fits. WC 1σ (thick line) and 2σ (thin line) uncertainty intervals are shown for the case where the other WCs are profiled (in black), and the case where the other WCs are fixed at their SM values of zero (in red).

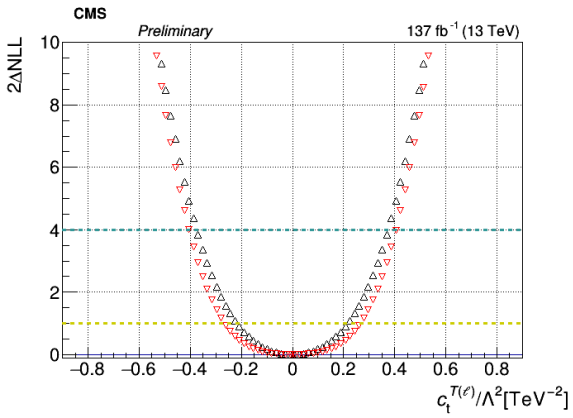
CMS
Preliminary
137 fb^{-1} (13 TeV)
2ΔNLL
$c_t^{T(\ell)}/\Lambda^2$[TeV^{-2}]

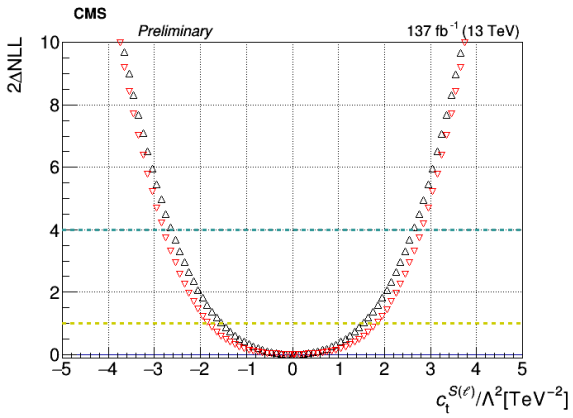
CMS
Preliminary
137 fb^{-1} (13 TeV)
2ΔNLL
$c_t^{S(\ell)}/\Lambda^2$[TeV^{-2}]

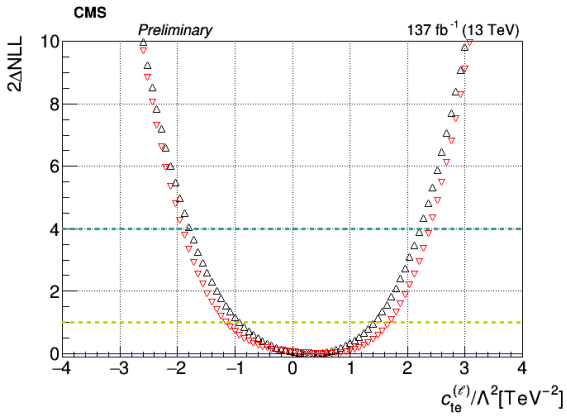
CMS
Preliminary
137 fb^{-1} (13 TeV)
2ΔNLL
$c_{te}^{(\ell)}/\Lambda^2$[TeV^{-2}]

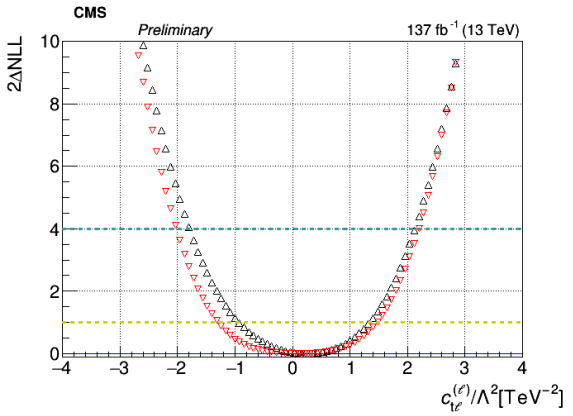
CMS
Preliminary
137 fb^{-1} (13 TeV)
2ΔNLL
$c_{t\ell}^{(\ell)}/\Lambda^2$[TeV^{-2}]

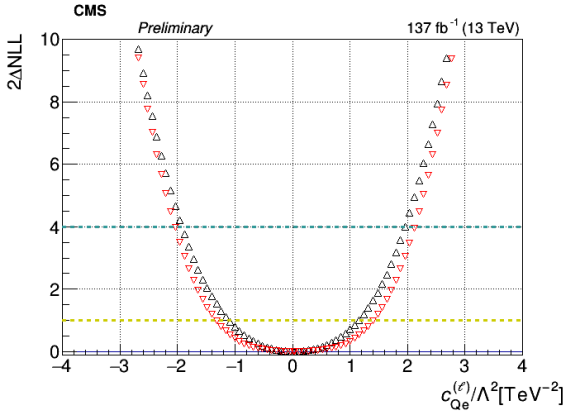
CMS
Preliminary
137 fb^{-1} (13 TeV)
2ΔNLL
$c_{Qe}^{(\ell)}/\Lambda^2$[TeV^{-2}]

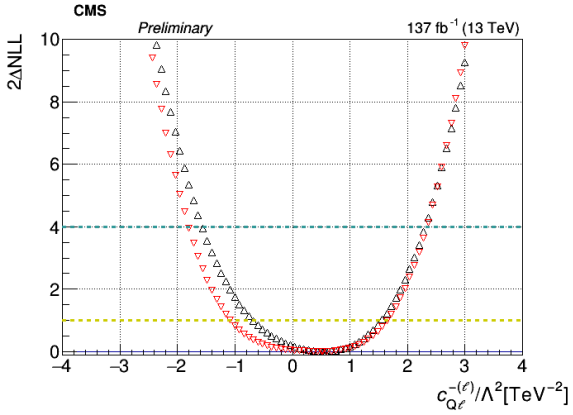
CMS
Preliminary
137 fb^{-1} (13 TeV)
2ΔNLL
$c_{Q\ell}^{-(\ell)}/\Lambda^2$[TeV^{-2}]

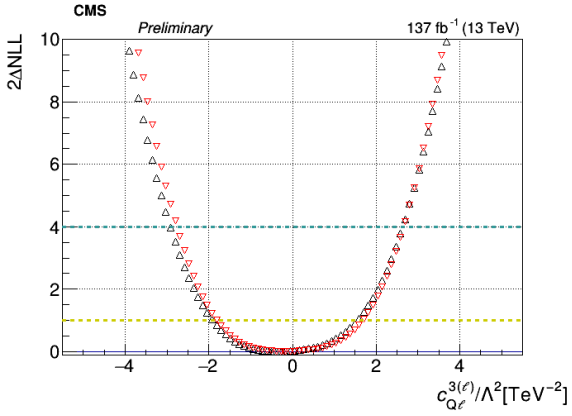
CMS
Preliminary
137 fb^{-1} (13 TeV)
2ΔNLL
$c_{Q\ell}^{3(\ell)}/\Lambda^2$[TeV^{-2}]

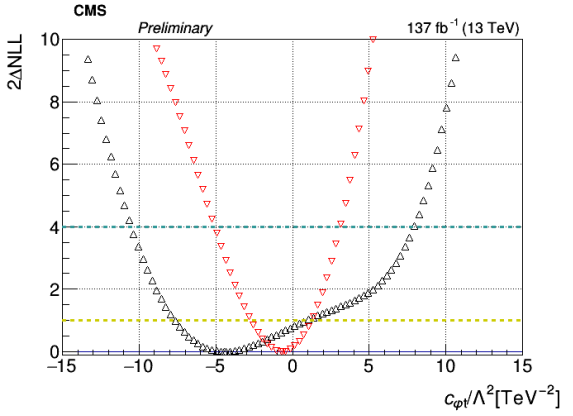
CMS
Preliminary
137 fb^{-1} (13 TeV)
2ΔNLL
$c_{\varphi t}/\Lambda^2$[TeV^{-2}]

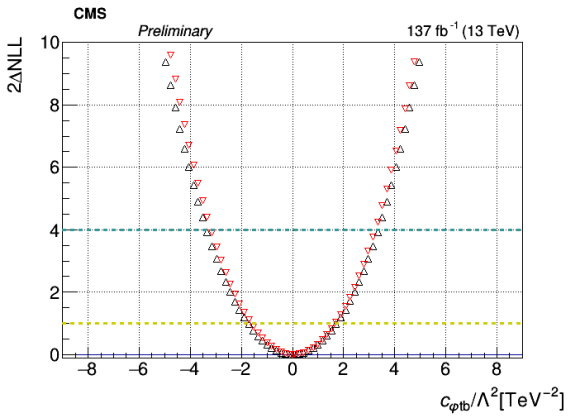
CMS
Preliminary
137 fb^{-1} (13 TeV)
2ΔNLL
$c_{\varphi tb}/\Lambda^2[\mathrm{TeV}^{-2}]$

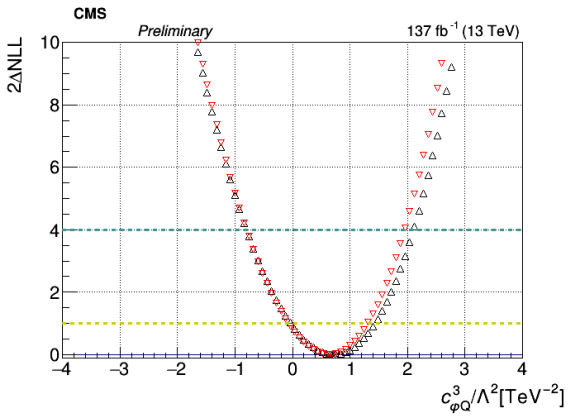
CMS
Preliminary
137 fb^{-1} (13 TeV)
2ΔNLL
$c^3_{\varphi Q}/\Lambda^2[\mathrm{TeV}^{-2}]$

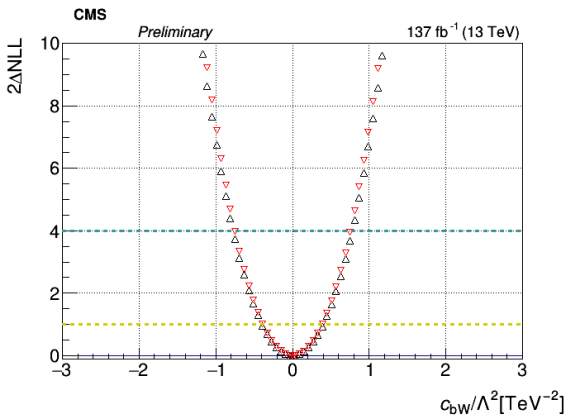
CMS
Preliminary
137 fb^{-1} (13 TeV)
2ΔNLL
$c_{bW}/\Lambda^2[\mathrm{TeV}^{-2}]$

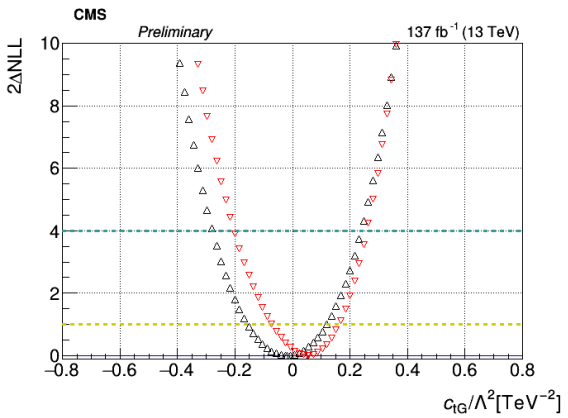
CMS
Preliminary
137 fb^{-1} (13 TeV)
2ΔNLL
$c_{tG}/\Lambda^2[\mathrm{TeV}^{-2}]$

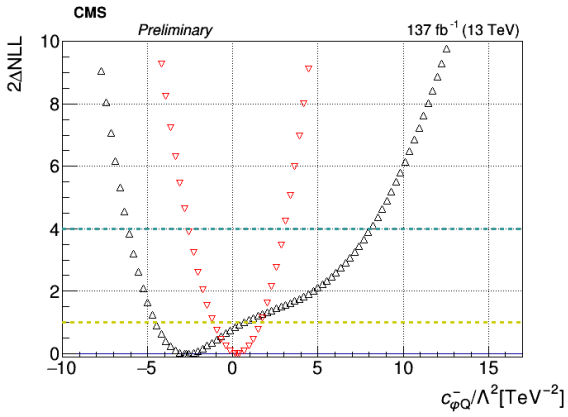
CMS
Preliminary
137 fb^{-1} (13 TeV)
2ΔNLL
$c^-_{\varphi Q}/\Lambda^2[\mathrm{TeV}^{-2}]$

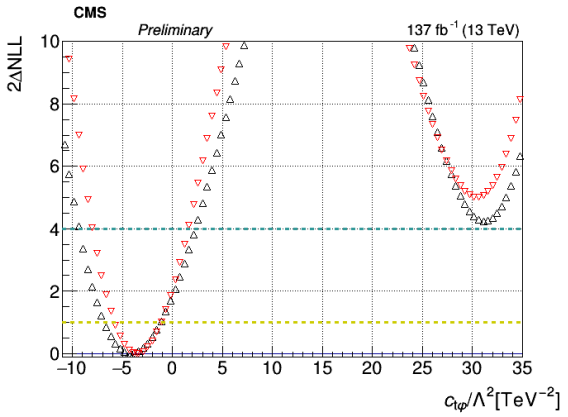
CMS
Preliminary
137 fb^{-1} (13 TeV)
2ΔNLL
$c_{t\varphi}/\Lambda^2[\mathrm{TeV}^{-2}]$

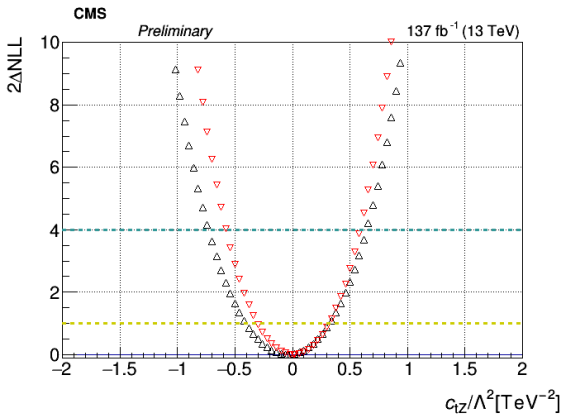
CMS
Preliminary
137 fb^{-1} (13 TeV)
2ΔNLL
$c_{tZ}/\Lambda^2[\mathrm{TeV}^{-2}]$

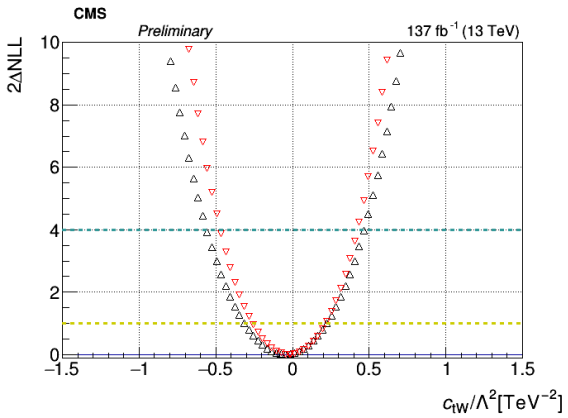
CMS
Preliminary
137 fb^{-1} (13 TeV)
2ΔNLL
$c_{tW}/\Lambda^2[\mathrm{TeV}^{-2}]$

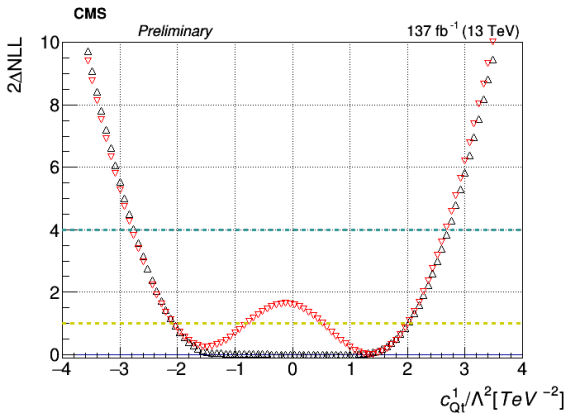
CMS
Preliminary
137 fb^{-1} (13 TeV)
2ΔNLL
$c^{1}_{Qt}/\Lambda^2[TeV^{-2}]$

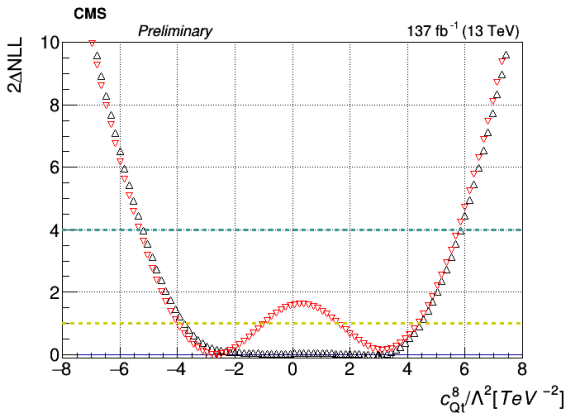
CMS
Preliminary
137 fb^{-1} (13 TeV)
2ΔNLL
$c^{8}_{Qt}/\Lambda^2[TeV^{-2}]$

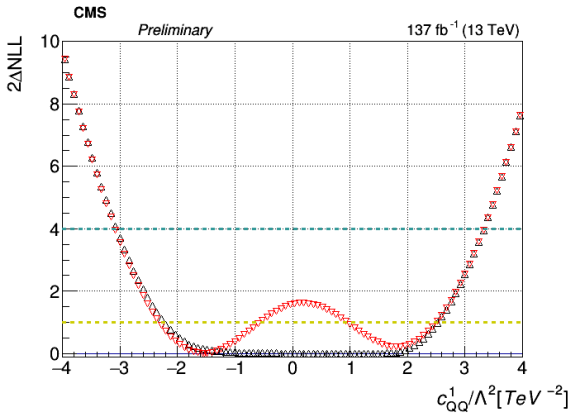
CMS
Preliminary
137 fb^{-1} (13 TeV)
2ΔNLL
$c^{1}_{QQ}/\Lambda^2[TeV^{-2}]$

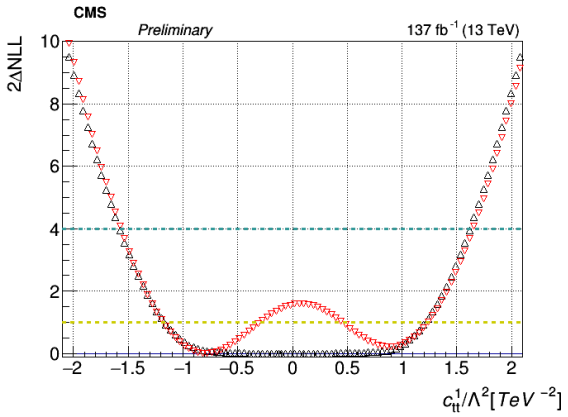
CMS
Preliminary
137 fb^{-1} (13 TeV)
2ΔNLL
$c^{1}_{tt}/\Lambda^2[TeV^{-2}]$

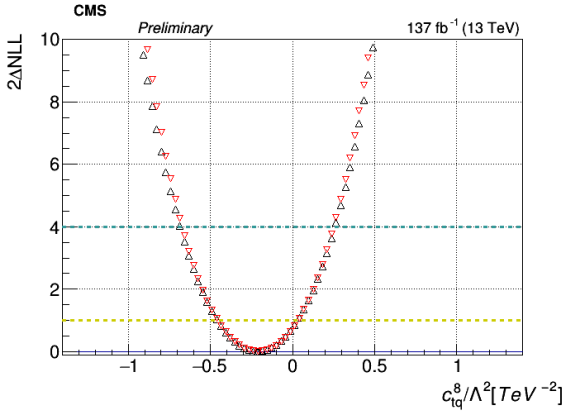
CMS
Preliminary
137 fb^{-1} (13 TeV)
2ΔNLL
$c^{8}_{tq}/\Lambda^2[TeV^{-2}]$

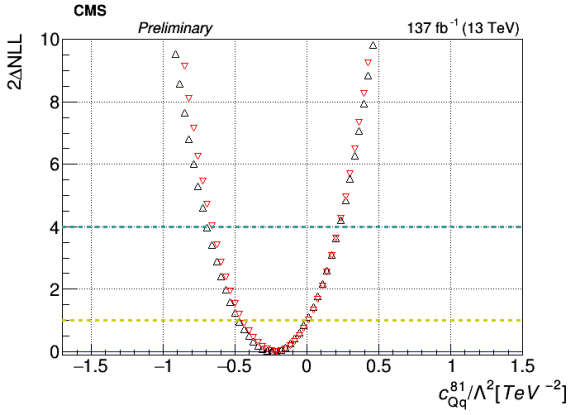
CMS
Preliminary
137 fb^{-1} (13 TeV)
2ΔNLL
$c^{81}_{Qq}/\Lambda^2[TeV^{-2}]$

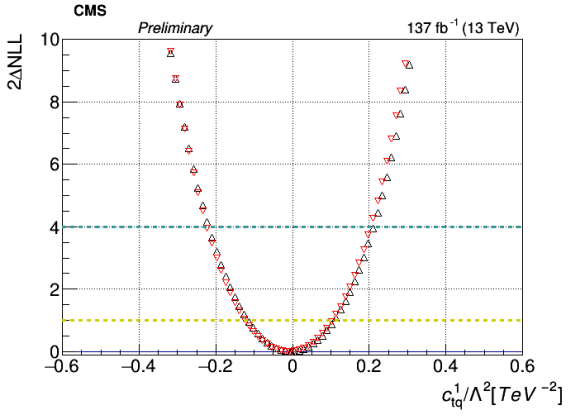
CMS
Preliminary
137 fb^{-1} (13 TeV)
2ΔNLL
$c^{1}_{tq}/\Lambda^2[TeV^{-2}]$

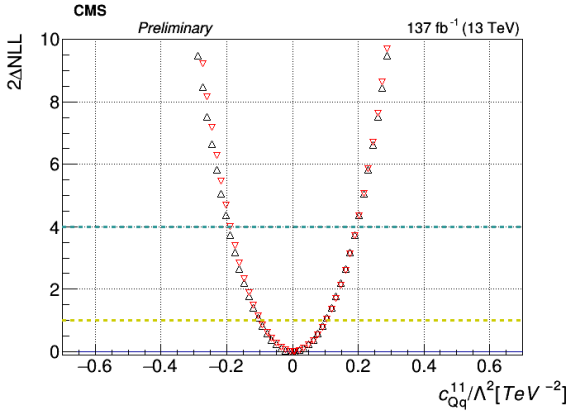
CMS
Preliminary
137 fb^{-1} (13 TeV)
2ΔNLL
$c^{11}_{Qq}/\Lambda^2[TeV^{-2}]$

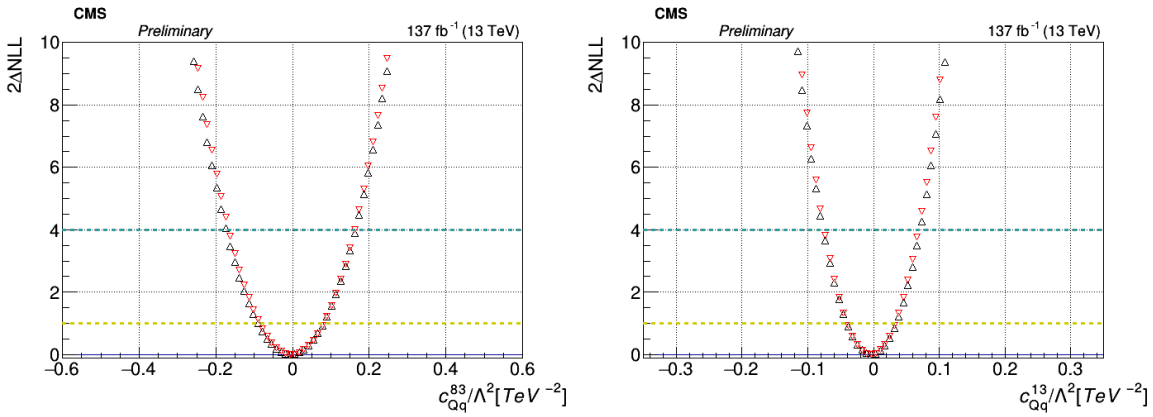

Figure 11.3. Observed 2ΔNLL values for 1d scans for each WCs. The 2ΔNLL values represented in black correspond to the case where the other WCs are profiled, while the 2ΔNLL values represented in red correspond to the case where the other WCs are fixed at their SM values of zero.

TABLE 11.2

OBSERVED 2σ UNCERTAINTY INTERVALS FOR THE 1D SCANS.

WC/Λ^2 [TeV^{-2}]	2σ Interval (others profiled)	2σ Interval (others fixed to SM)
$c_t^{T(\ell)}$	[-0.37, 0.37]	[-0.41, 0.41]
$c_t^{S(\ell)}$	[-2.63, 2.63]	[-2.81, 2.81]
$c_{te}^{(\ell)}$	[-1.79, 2.22]	[-1.92, 2.39]
$c_{t\ell}^{(\ell)}$	[-1.79, 2.13]	[-2.02, 2.20]
$c_{Qe}^{(\ell)}$	[-1.92, 1.96]	[-2.05, 2.13]
$c_{Q\ell}^{-(\ell)}$	[-1.57, 2.31]	[-1.81, 2.34]
$c_{Q\ell}^{3(\ell)}$	[-2.92, 2.64]	[-2.77, 2.66]
$c_{\varphi t}$	[-10.51, 7.94]	[-5.09, 3.11]
$c_{\varphi tb}$	[-3.36, 3.36]	[-3.19, 3.24]
$c_{\varphi Q}^{3}$	[-0.80, 2.11]	[-0.80, 1.95]
c_{bW}	[-0.77, 0.78]	[-0.75, 0.76]
c_{tG}	[-0.28, 0.24]	[-0.20, 0.26]
$c_{\varphi Q}^{-}$	[-6.14, 8.10]	[-2.61, 3.02]
$c_{t\varphi}$	[-9.34, 2.30]	[-8.00, 1.57]
c_{tZ}	[-0.73, 0.65]	[-0.58, 0.59]
c_{tW}	[-0.56, 0.47]	[-0.47, 0.42]
c_{Qt}^{1}	[-2.75, 2.71]	[-2.79, 2.67]
c_{Qt}^{8}	[-5.21, 5.85]	[-5.33, 5.76]
c_{QQ}^{1}	[-3.06, 3.33]	[-3.09, 3.33]
c_{tt}^{1}	[-1.58, 1.62]	[-1.57, 1.65]
c_{tq}^{8}	[-0.68, 0.26]	[-0.67, 0.25]
c_{Qq}^{18}	[-0.69, 0.22]	[-0.66, 0.22]
c_{tq}^{1}	[-0.22, 0.21]	[-0.22, 0.20]
c_{Qq}^{11}	[-0.19, 0.19]	[-0.19, 0.20]
c_{Qq}^{38}	[-0.17, 0.16]	[-0.17, 0.16]
c_{Qq}^{31}	[-0.08, 0.07]	[-0.08, 0.07]

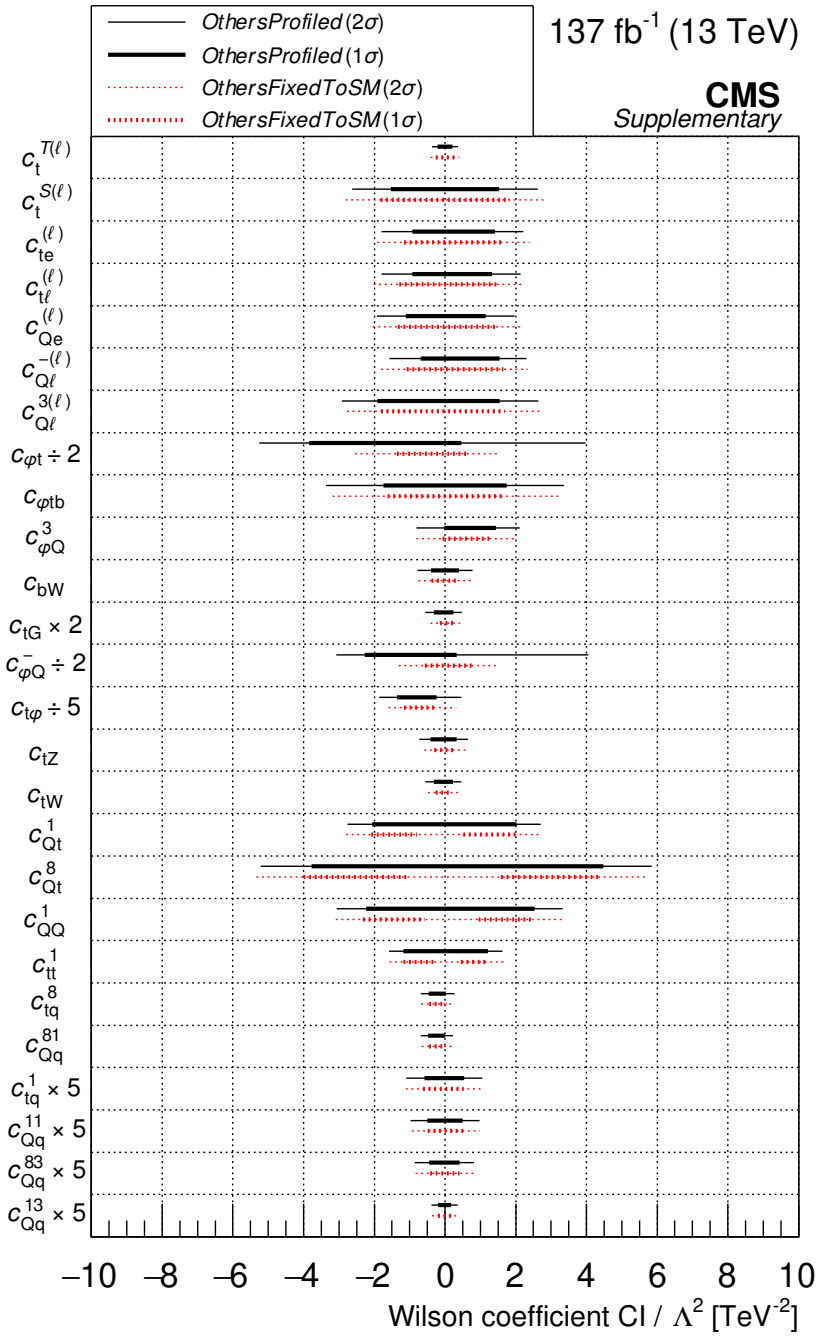

Figure 11.4. Summary of limits from fits to data. WC 1σ (thick line) and 2σ (thin line) uncertainty intervals are shown for the case where the other WCs are profiled (in black), and the case where the other WCs are fixed at their SM values of zero (in red).

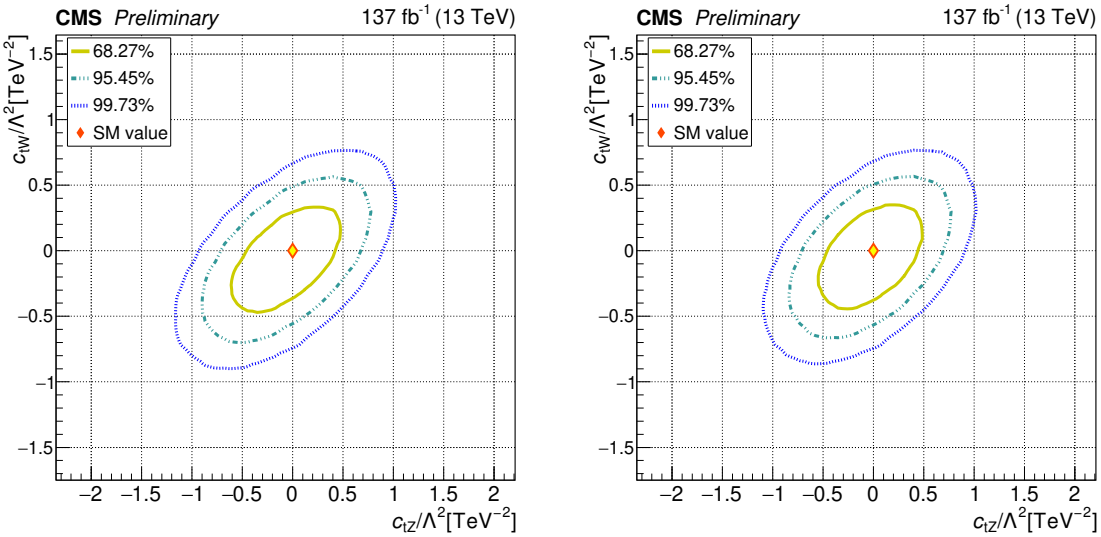

Figure 11.5. The observed 68%, 95%, and 99.7% confidence contours from the 2-dimensional scan over c_{tZ} and c_{tW} with the other 24 WCs profiled (left), and fixed to their SM values (right). The SM prediction is indicated with the diamond-shaped marker.

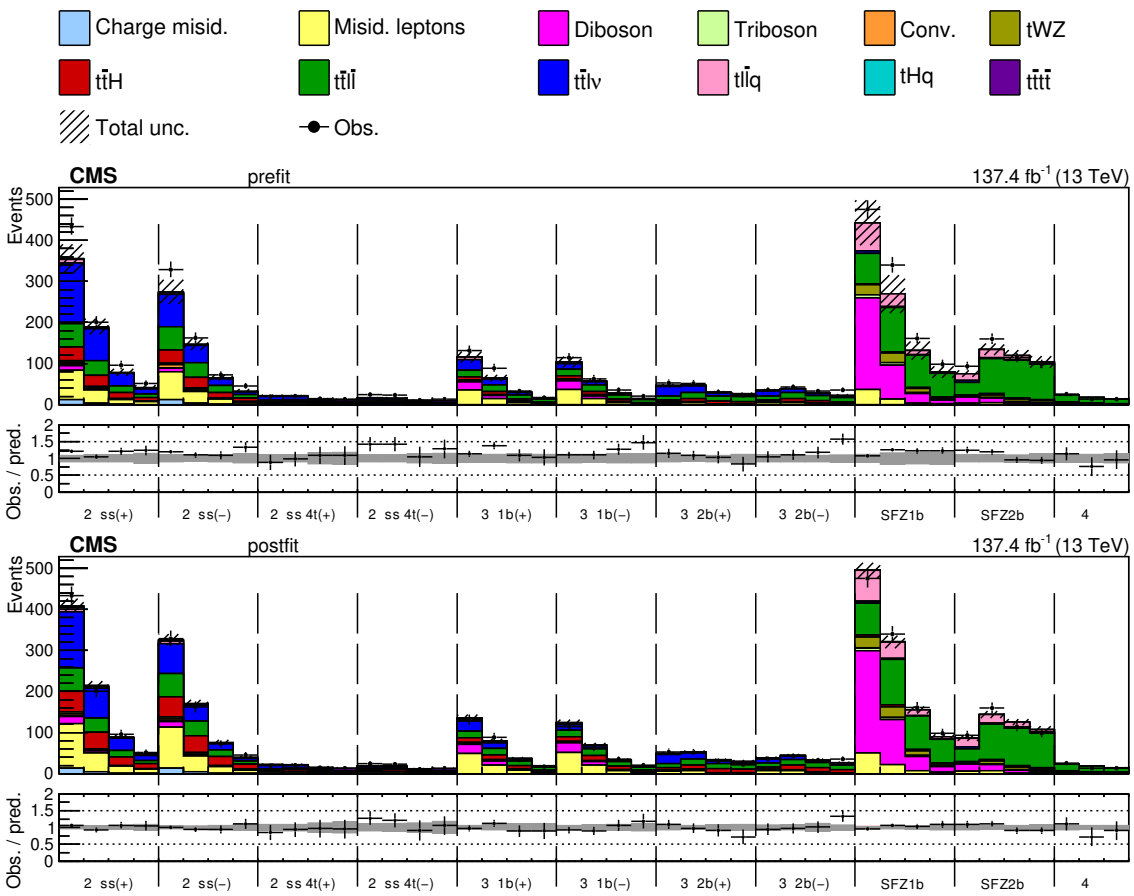

Figure 11.6. The observed yields and the predicted prefit (top) and postfit (bottom) yields. As explained in the text (Section 11.3), in the prefit case the predicted yields have been reweighted to the SM, while in the postfit case the predicted yields have been reweighted to the best fit point from the unblind fits. Here we have integrated over the kinematic variables, so the bins in these histogram correspond to the jet multiplicity categories of the analysis categories.